Applied Catalysis A: General 524 (2016) 173–181

Contents lists available at ScienceDirect

Applied Catalysis A: General

journal homepage: www.elsevier.com/locate/apcata

Porous aluminosilicate inorganic polymers (geopolymers): a new class of environmentally benign heterogeneous solid acid catalysts

Mohammad I.M. Alzeer[a,b,*], Kenneth J.D. MacKenzie[a,b], Robert A. Keyzers[a]

[a] School of Chemical and Physical Sciences, Victoria University of Wellington, P.O. Box 600 Wellington, New Zealand
[b] MacDiarmid Institute for Advanced Materials and Nanotechnology, New Zealand

ARTICLE INFO

Article history:
Received 13 March 2016
Received in revised form 15 June 2016
Accepted 17 June 2016
Available online 23 June 2016

Keywords:
Beckmann rearrangement
cyclohexanone oxime
caprolactam
geopolymer
catalysis

ABSTRACT

Aluminosilicate inorganic polymers (geopolymers) were developed as a new class of cost-efficient, environmentally friendly, solid acid catalysts and their performance evaluated in a model liquid-phase Beckmann rearrangement reaction (cyclohexanone oxime to ε-caprolactam). The active sites were generated within the structure of the geopolymers by ion-exchange with NH_4^+ followed by thermal treatment. The effect of varying the starting composition on the textural and acidic properties of the geopolymer catalysts was studied and its influence on the catalytic activity was investigated. Catalytic performance was significantly improved by the use of post-synthetic treatments. No significant decrease in the yield of ε-caprolactam after recycling for five times suggesting that geopolymer-based catalysts are advantageous over supported catalysts which often lose their catalytic activity due to leaching of the active sites from the support. The catalytic activities obtained in this study are comparable, and sometimes superior, to other solid catalysts suggesting that geopolymers have a great potential as environmentally benign heterogeneous catalysts.

1. Introduction

The Beckmann rearrangement is a ubiquitous reaction vital to many industrially important organic syntheses. One such reaction is the production of ε-caprolactam, the precursor of polyamide-6 (nylon-6), which is produced in vast amounts; in 2012 alone, five million metric tonnes of caprolactam were produced [1]. The industrial synthesis of caprolactam is by a one-pot ammoximation of cyclohexanone, followed by the Beckmann rearrangement of the cyclohexanone oxime using concentrated sulphuric acid and/or oleum as the catalyst and solvent [2]. Each tonne of caprolactam produced in this process produces two tonnes of ammonium sulfate waste, formed by neutralisation of the acid with ammonia [3]. Generation of such large amounts of waste presents serious environmental problems and expense involved in its treatment and disposal. Recent increased environmental awareness and the stimulus of greener chemistry has driven the rapid development of new heterogeneous catalysts for a wide range of organic synthesis applications [4].

Solid acid catalysts are reusable, easy to separate from the reaction mixture and usually generate less by-products [5]. Several of the heterogeneous catalysts employed for the gas phase Beckmann rearrangement of cyclohexanone oxime to ε-caprolactam, Scheme 1, during the last three decades include zeolites (mainly high silicon MFI framework structures [6–8] and nanosheets [9]), molecular sieves [10,11] and functionalised oxides or mixed oxides [12,13]. Large-scale production of ε-caprolactam (~90000 tonnes/year) by the Beckmann rearrangement in the gas phase was achieved in 2003 by the Sumitomo Corporation, Japan, using H-ZSM-5 zeolite as the catalyst [14]. However, such vapour-phase systems suffer the drawbacks of requiring high temperatures (often > 623 K) which can also deactivate the catalyst by facilitating side reactions such as polymerisation, with a deleterious effect on the catalyst life time and reusability [1,15–20]. Although the reusability problem can be solved by introducing into the reaction system an additional fluidized-bed reactor for regenerating the catalyst while conducting the reaction [14], such systems are energy consuming. Thus, for both economic and environmental reasons, interest has recently increased in the liquid-phase Beckmann rearrangement of cyclohexanone oxime. Various heterogeneous catalysts have been proposed for this purpose, including zeolites (mainly large pore Y and beta type zeolites [15–17]), molecular sieves [1,21,22], mixed oxides [18,23,24], heteropolyacids [19], MOFs [20] and ionic liquids [25].

The nature and the location of the active sites responsible for catalysing the Beckmann rearrangement reaction are in some

* Corresponding author.

http://dx.doi.org/10.1016/j.apcata.2016.06.024
0926-860X/

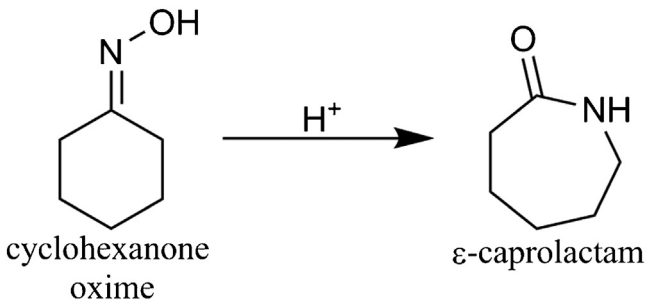

Scheme 1. xxx.

dispute in the literature. Some reports suggest that the rearrangement is catalysed by Bronsted acid sites located inside the pores of a ZSM-5 zeolite catalyst [26,27], whereas other studies have implicated the strong acidic bridging hydroxyl groups in the strong adsorption of the product to the catalyst, giving rise to its rapid deactivation [28]. However, a more recent general consensus is that the most likely active sites for this rearrangement are the non- or weakly acidic hydrogen-bonded silanol groups (silanol nests) and vicinal silanols located on the outer surface of the catalyst or just under the mouths of the pores [12–14]. Non-acidic silanol groups (isolated Si-OH) located on the outer surface of zeolite nanosheets have also been reported to be active sites for this reaction [9]. The mechanism of the Beckmann rearrangement over solid heterogeneous catalysts and the effect of the solvent type have been reviewed elsewhere [28,29].

The application of solid catalysts for Beckmann rearrangements in the liquid phase is very limited compared with vapour-phase systems. Zeolites suffer from the constraints imposed by the size of their micropores which hinders their efficiency in liquid phase systems by diffusional limitations which cause deactivation and affect the catalyst life time [9,30]. Although mesoporous silicates or molecular sieves (M41S) do not suffer from mass-transfer constraints, they have low hydrothermal stability and low acidity and their synthesis involves the use of costly and sometimes toxic organic structure-directing agents (OSDAs) and lengthy thermal treatments [31–33]. These drawbacks have hindered their use in large scale applications.

Thus, there is still a need for new cost-efficient heterogeneous solid catalysts that are also environmentally benign. Here we report the development and performance of a new class of porous aluminosilicate inorganic polymers (geopolymers) that are easily and cheaply synthesised, environmentally-friendly and with acidic properties that can readily be tailored to the requirements for heterogeneous solid acid catalysis in fine chemical applications.

Geopolymers have been described as amorphous fine-grained analogues of zeolites [34]. Unlike amorphous silica alumina (ASA) that consists of different forms of Al (mainly octahedral and Al_2O_3) grafted into a silica backbone, the geopolymer structure consists of three-dimensional random arrangements of tetrahedral silicate and aluminate units joined through their common oxygen atoms. Charge balance in the tetrahedral aluminate units is achieved by the presence of (usually) monovalent alkali ions that give the geopolymer zeolite-like ion-exchange properties [35]. Historically, geopolymers have been used as ecologically-friendly substitutes for Portland cement, but more recently their ability to be functionalised has led to a range of more advanced applications such as drug delivery agents, photocatalysts and precursors to advanced ceramics [36].

The possible use of geopolymers as a new class of environmentally-friendly heterogeneous solid catalysts arises from their facile and energy-efficient synthesis from simple raw materials (kaolin clay or industrial wastes such as fly ash), the ability to tailor their porosity to form micro, meso, or even hierarchical structures without using conventional expensive and/or toxic OSDAs [37,38], and the ability to control their acidity and incorporate versatile active sites into their structures either by ion-exchange or metal substitution of the Si or Al in the geopolymer framework [39]. Despite these interesting features, there are only very few reports of geopolymer-based catalysts; Sazama et al. [40] have reported the use of geopolymers as redox catalysts for the reduction of NOx by ammonia and the oxidation of volatile hydrocarbons where the active catalyst was Pt, Fe, Cu or Co, supported or ion-exchanged on a geopolymer matrix. Geopolymers have also used to support other catalytic nanoparticles such as TiO_2 [41] and CuO [42] for the photocatalytic applications. Sharma and co-workers have also reported the use of geopolymers loaded with Ca^{2+} as base catalysts for the generation of biofuel [43]. However, no workers have reported the use of geopolymers into which suitable solid acidity was incorporated into the structure for catalysing industrially important organic reactions such as the Beckmann rearrangement of cyclohexanone oxime to ε-caprolactam.

In the present work, geopolymers were developed as new solid acid catalysts with active sites generated within the structure of the geopolymer itself, rather than using the geopolymer framework as a catalyst support. The nature of these acid sites was investigated, and the catalytic activity was evaluated in a liquid-phase Beckmann rearrangement of a model system (rearrangement of cyclohexanone oxime to ε-caprolactam). The effect of varying the preparation compositions on the textural and acidic properties of the geopolymers was studied and its influence on the catalytic activity was examined. Post-synthetic treatments to improve the catalytic performance of the prepared catalysts were also developed, and their performance over multiple reaction cycles evaluated. The performance of the geopolymer catalysts was compared with zeolites Y and ZSM-5, and with other catalysts that have been reported under identical reaction conditions.

2. Experimental

2.1. Geopolymer synthesis

The geopolymers were prepared from New Zealand kaolinite-type halloysite clay (Imerys Premium Grade), the chemical composition of which is shown in Table 1.

Table 1
Composition of halloysite.

Oxide	% wt.
SiO_2	49.5
Al_2O_3	35.5
Fe_2O_3	0.29
TiO_2	0.09
K_2O	0.01
Na_2O	0.04
CaO	0.02
MgO	0.02
L.O.I.	13.8

The clay was dehydroxylated at 600 °C for 12 hr. and gradually mixed with an aqueous solution of analytical grade NaOH or KOH (Panreac) and sodium silicate (FERNZ Chemical Co, NZ, Type "D", Na_2O/SiO_2 = 0.48, solids content = 41.1 mass %) or potassium silicate (Type K66, Ineos Silicas, UK), depending on whether the sodium or potassium form of the geopolymer was being synthesized. Two sodium and two potassium-based geopolymers were prepared with "normal" composition (e.g. SiO_2/Al_2O_3 ~3.5), designated Na-N and K-N, and two other compositions, containing

Table 2
Molar ratios of the geopolymers[a].

Geopolymer	SiO_2/Al_2O_3	H_2O/Al_2O_3	Na_2O/Al_2O_3	K_2O/Al_2O_3
K-N	3.59	13.26	0.02	1.11
K-hiSi	5.19	14.81	0.02	1.30
Na-N	3.54	13.59	1.26	0.01
Na-hiSi	6.40	22.88	2.27	0.0006
Na-hiSi-Seq[b]	7.62	22.88	0.0002	0.0006

[a] determined by XRF analysis.
[b] ion-exchanged with NH_4^+.

double this amount of silica, designated Na-hiSi and K-hiSi were also prepared. The molar compositions of all these samples are shown in Table 2. The compositions of the high-silica geopolymers were adjusted by the addition of fine silica fume (Elkem 971-U, Elkem, Norway) simultaneously with the clay. After thorough mixing for 10 min. the geopolymer resins were cured in covered plastic molds at 80 °C for 6 hr., then uncovered and oven-dried at 40 °C overnight. The hardened blocks were then broken into pieces and ground in a vibratory mill (Bleuler, Switzerland) fitted with a tungsten carbide pot and milling rings and sieved to pass a 105 μm mesh.

2.2. Catalyst preparation

The alkali ions of the geopolymers prepared as above were exchanged with NH_4^+ by the method of O'Connor et al. [35]. One gram of geopolymer powder was treated with 100 ml of 0.1 M NH_4Cl solution (Panreac) with vigorous stirring at room temperature for 12 hr., and then washed thoroughly with a freshly prepared solution of 0.1 M NH_4Cl, filtered, then washed thoroughly with distilled water to remove any remaining alkali ions and dried at 40 °C overnight. The zeolites Y and ZSM-5 used for comparison purposes in the catalytic reactions were ion-exchanged in the same manner.

2.3. Sequential post-synthetic treatment

In some cases, the geopolymers were sequentially dealuminated and desilicated after ion exchange, by the procedure of Verboekend et al. [33] in which a weighed amount of the geopolymer catalyst was first dealuminated by treatment with 20 ml/g 0.11 M Na_2H_2 EDTA (Merck) for 5 hr. at 85 °C. This was followed by desilication by treatment with 30 ml/g 0.1 M NaOH for 30 min at 65 °C in a plastic container placed in a thermostatic bath. The third step of the treatment was an acid wash, performed as in the first dealumination but for only 2 hr. Between each of these steps, the solid was filtered, washed with distilled water and dried at 50 °C overnight. Finally these samples were exchanged with NH_4^+ as described above, but in three 6-hr. treatments with NH_4Cl solution. The geopolymer samples treated in this way are designated Seq (e.g. Na-hiSi-Seq). It should be noted that only the results for the Na-hiSi samples subjected to this post-synthetic treatment are presented here since these produced superior catalytic performance.

2.4. Catalyst characterization

The formation of the geopolymer was confirmed by X-ray powder diffraction (Bruker D8 Avance X-ray diffractometer with Ni-filtered Cu Kα radiation operated at 45 kV and 40 mA.). ^{27}Al and ^{29}Si solid-state magic angle spinning nuclear magnetic resonance (MAS NMR) spectra were acquired at a magnetic field of 11.7 T using a Bruker Avance III 500 spectrometer operating at a ^{27}Al frequency of 130.24 MHz and a ^{29}Si frequency of 99.29 MHz. The 11.7 T ^{27}Al solid-state spectra were acquired using a 4 mm Doty MAS probe with a silicon nitride rotor spun at 10–12 kHz, a 1 μs pulse and a 1 s recycle time, the spectra referenced with respect to $Al(H_2O)^{3+}$. The ^{29}Si spectra were acquired with a 5 mm Doty MAS probe and a zirconia rotor spun at ~6 kHz. The excitation pulse for ^{29}Si was 7 μs with a recycle time of 30 s and the spectra were referenced with respect to tetramethylsilane (TMS).

The N_2 adsorption-desorption isotherms were measured at −196 °C using a Micromeritics ASAP 2010. All the samples were degassed at 110 °C to 3 mTorr pressure using the instrument's degassing system. The specific surface area was measured by the Brunauer–Emmett–Teller (BET) method over a p/p° range of 0.05-0.3. The total pore volume was measured by single point adsorption at $p/p^\circ = 0.995$. The mesopore volumes and the average adsorption pore widths were determined by the Barrett-Joyner-Halenda (BJH) method. Transmission electron microscopy (TEM) was carried out using a JEOL 2010 transmission electron microscope operated at 200 kV.

The ion-exchange process was monitored by FTIR in which the powder samples were suspended in a KBr disk and the spectra acquired using a Perkin Elmer Spectrum One FTIR spectrometer in the range 4000–450 cm^{-1}. A quantitative analysis of the amount of pyridine adsorbed was obtained by thermogravimetric analysis (TGA) using a Shimadzu TGA-50 thermal analyser at a heating rate of 10 °C min^{-1} up to 800 °C in flowing air (50 ml min^{-1}). The difference in the weight loss between the sample with and without pyridine indicated the total content of acid sites in the sample (see supporting information (SI), Fig. SI3). The adsorption-desorption of pyridine on the catalyst surface was carried out as follows: 0.1 g of the catalyst was heated to 450 °C for 10 min then degassed at 250 °C for 12hr. at 200 mTorr vacuum using a Micromeritics VacPrep061 sample degassing system. The powder then was left to cool to room temperature and exposed to pyridine at 150 °C for 1 hr. to allow the surface to become saturated. The physisorbed pyridine was then desorbed at 100 °C for 1 hr. under the same vacuum conditions. The nature of the active sites was further investigated by FTIR spectroscopy of the adsorbed pyridine (see Fig. SI2).

2.5. Catalytic activity

The rearrangement of cyclohexanone oxime to ε-caprolactam was carried out in a magnetically stirred 50-ml two-necked round bottom flask equipped with a reflux condenser and placed in a thermostatic bath. In a typical run 0.1 g of cyclohexanone oxime was dissolved in 20 ml solvent (benzonitrile) and heated to 100 °C followed by the addition of 0.1 g of the catalyst and the reaction temperature was set at 130 °C under atmospheric pressure for 5 hr. (wt.% 1:200:1 respectively). The catalysts were the NH_4^+-ion-exchanged form of the geopolymers, heated at 450 °C for 10 min prior to the reaction which was monitored by periodic sampling in which 0.1 ml samples were taken and analysed using a Shimadzu QP20-Plus GC–MS with a 30 meter Rxi-5sil MS capillary column (Full details of the GC–MS method are reported in the SI). Calibration curves covering the range of 0.044–0.009 mmol/ml of each reactant and product were used for quantitative analysis. Each reaction was repeated at least three times and the reproducibility is expressed in the form of standard errors that were measured at the conclusion of each reaction. The conversion and selectivity of the reaction were determined according to the IUPAC recommendations [44] as follows:

$$Conversion\% = \frac{\text{amount of oxime converted}}{\text{amount of oxime fed}} x100\%$$

Where the amount of oxime converted = the amount fed − the amount left over.

$$Selectivity\% = \frac{\text{amount of product formed}}{\text{amount of oxime converted}} x100\%$$

$$Mass\ balance\% = \frac{\text{sum of all productsformed} + \text{amount of oxime remained}}{\text{amount of oximefed}} x100\%$$

To evaluate the reusability of the catalyst, the catalyst was transferred quantitatively to a centrifuge tube after each reaction experiment and separated from the reaction solution. The solid catalysts were then washed twice with 2 ml acetone which was combined and analysed by GC-MS to identify and quantify any adsorbed reactant or product on the surface of the catalyst; the amounts of these components were combined with those of the primary catalytic results. After washing with acetone, the catalyst was dried at ~50 °C overnight then heated at 450 °C for 10 min prior to each reaction cycle. The structural stability of the spent geopolymer-based catalyst was evaluated by XRD and FTIR after 5 reaction cycles.

3. Results and Discussion

3.1. Catalyst characteristics

XRD traces of the synthesised catalyst powders are shown in Fig. 1. All the geopolymers show the broad background amorphous feature from 20–40° 2θ typical of well-formed geopolymers on which are superimposed two sharp reflections arising from crystalline silica polymorphs quartz and cristobalite present as impurities in the original clay. Traces of $Na_2CO_3.H_2O$ are also present, arising from the reaction of NaOH with atmospheric CO_2; this is most evident in the Na-hiSi sample (Fig. 1d) which contains the highest Na_2O content (Table 2). The post synthetic treated geopolymer (Fig. 1e) shows a slight shift of the broad hump which may be due to washing out some of the crystalline phases and Al-rich debris. The XRD patterns of these geopolymers are unchanged by thermal treatment (see Fig. SI1).

Solid-state ^{27}Al and ^{29}Si MAS NMR spectra are shown in Fig. 2. The chemical shifts of the Al spectra indicate the coordination number of the aluminium, which in well-formed geopolymers is almost entirely 4; this is seen to be the case in the spectra of all the

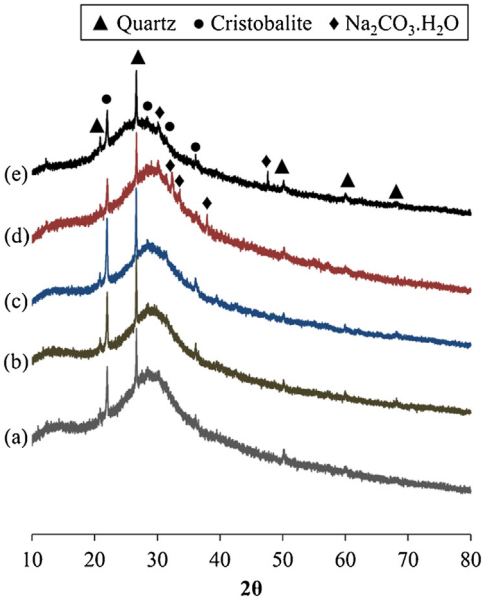

Fig. 1. XRD traces of the prepared and the post synthetic treated geopolymers. (a) K-hiSi, (b) K-N, (c) Na-N, (d) Na-hiSi, (e) Na-hiSi-Seq.

geopolymers in which the chemical shift of the principal resonance is typically tetrahedral (~60 ppm) [45,46]. The slight shift to lower frequency in the hiSi geopolymers probably reflects their higher Si/Al ratio (Fig. 2a and d). Dealumination is also confirmed in the post-synthetic treated geopolymer by a further shift to 57.8 ppm (Fig. 2e). Two additional small, broad ^{27}Al resonances at about 4 ppm in the Na-geopolymer samples (Fig. 2c and d) arise from octahedrally-coordinated AlO_6 [46], indicating the presence of a small amount of unreacted clay mineral, in which the Al is in solely 6-fold coordination, but the absence of unreacted starting material in the K-based samples (Fig. 2a and b) indicates more complete geopolymer formation in these samples, as expected from previous

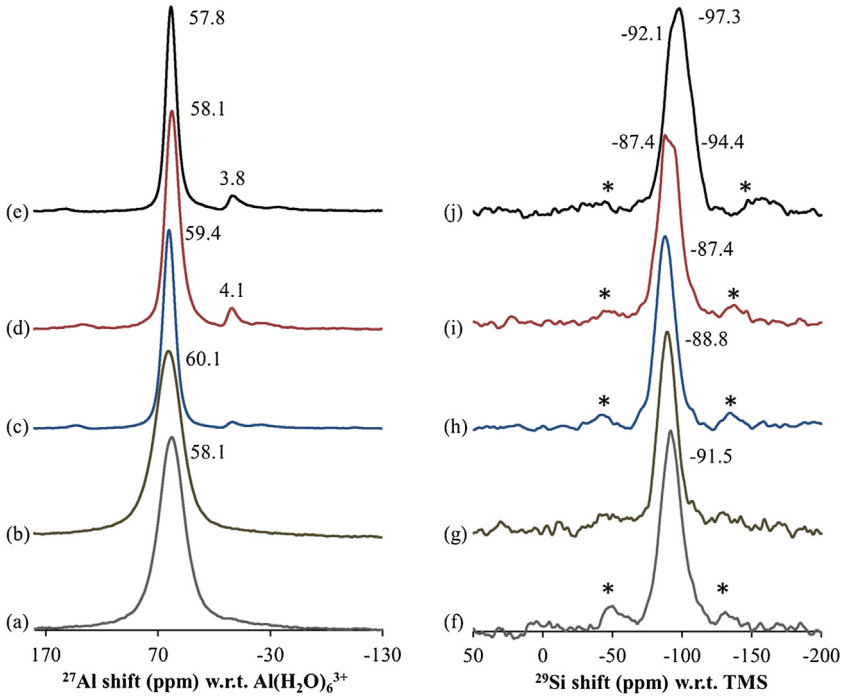

Fig. 2. (a)-(e) Representative ^{27}Al MAS NMR spectra of geopolymer catalysts. (a) K-hiSi, (b) K-N, (c) Na-N, (d) Na-hiSi, (e) Na-hiSi-Seq. (f)-(j) Representative ^{29}Si MAS NMR spectra of geopolymer catalysts. (f) K-hiSi, (g) K-N, (h) Na-N, (i) Na-hiSi, (j) Na-hiSi-Seq. The asterisks denote spinning side bands.

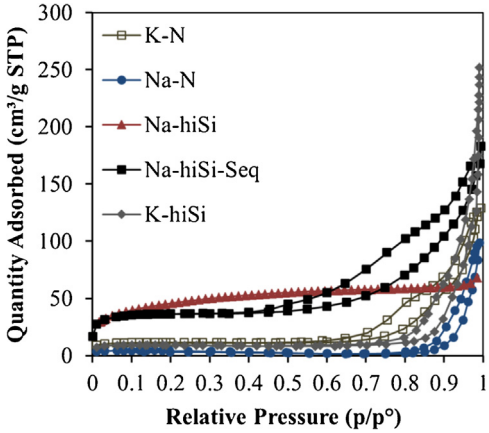

Fig. 3. N_2 adsorption-desorption isotherms of the geopolymer-based catalysts.

studies [45]. The ^{29}Si MAS NMR spectra of K-hiSi, K-N, and Na-N (Fig. 2f–h) shows a single broad resonance in the range 85–95 ppm, typical of a well-formed geopolymer containing tetrahedral Si coordinated to 4 Al atoms [46]. The Na-hiSi sample (Fig. 2i) contains an additional resonance at about −94.4 ppm, indicating the presence of Si (Q^3) surrounded by 3 Al [46]. The Na-hiSi-Seq sample (Fig. 2j) also contains these two resonances, but shifted to lower frequencies due to dealumination. By contrast with the Na-hiSi spectrum, the intensity of the Si Q^3 resonance at −97.3 ppm is greater than that of Si Q^4 at −92.1 ppm in the hiSi-Seq sample, reflecting a higher concentration of silanol groups formed in the post-synthetic treatment.

The N_2 adsorption-desorption isotherms of the catalysts are shown in Fig. 3 and the corresponding porosity values in Table 3. The Na-hiSi sample shows a type I isotherm typical of microporous materials, whereas all the other geopolymers show type IV isotherms with distinguishing hysteresis loops corresponding to mesoporous materials. Fig. 3 also shows that the sequential treatment was successful in introducing mesopores into the structure of Na-hiSi geopolymer.

The effect of the post-synthetic treatment on the porosity of the geopolymer catalysts of forming a mesoporous material with double the pore volume, pore width and surface area of the starting geopolymer is described in Table 3. Dealumination, either by thermal or acid treatments, is routinely employed in zeolitic materials to introduce secondary mesopores or remove the extra framework aluminium (EFAl) [47]. More recently, desilication by base treatment has been carried to introduce intracrystaline mesoporosity that cannot be achieved via dealumination [48]. Verboekend et al. [33] reported that dealumination followed by desilication (described as sequential treatment) also generates a range of silanol groups (isolated, bridging and silanol nests) in the aluminium-rich zeolite Y. In the present work, this same sequential treatment was applied to geopolymers to maximise the concentration of silanol groups formed and thereby improve the catalytic performance of the geopolymers.

Representative TEM micrographs of selected geopolymers (Fig. 4) show that K-hiSi contains large mesopores stacked over each other (Fig. 4a), whereas Na-hiSi (Fig. 4b) contains small randomly oriented non-uniform micropores. The post-synthetic sequential treatment results in the formation of ∼10 nm wide mesopores (Fig. 4c); interparticle voids are also observed in the Na-hiSi-Seq sample (Fig. 4d), explaining the high surface area resulting from the post synthetic treatment. This is consistent with the N_2 adsorption-desorption isotherm of this sample which shows an H3 type of hysteresis associated with particle aggregates, producing slit-like pores [49].

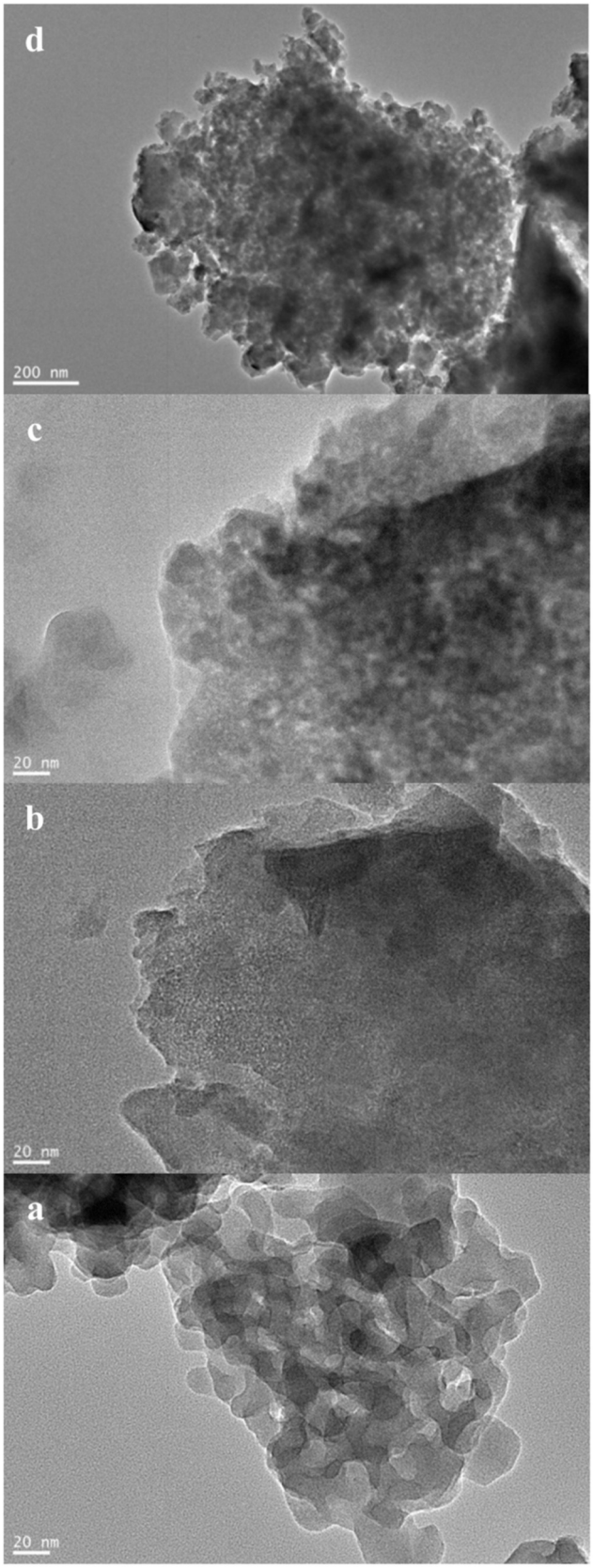

Fig. 4. Representative TEM micrographs of selected geopolymers. (a) K-hiSi, (b) Na-hiSi, (c,d) Na-hiSi-Seq.

Table 3
Textural and acidic properties of the various geopolymer-based catalysts.

Catalyst	Acid amount (mmol/g)[a]	S_{BET} (m^2/g)	V_{total} (cm^3/g)[b]	V_{meso} (cm^3/g)[c]	D_{pore} (nm)[c]
K-N	0.27	50.00	0.20	0.20	22.07
K-hiSi	0.30	40.20	0.39	0.39	50.20
Na-N	0.18	18.00	0.15	0.15	45.06
Na-hiSi	0.38	135.00	0.10	0.00	2.70
Na-hiSi-Seq	0.43	211.50	0.28	0.26	9.86

[a] total (determined from TGA profile of adsorbed pyridine, see Fig. SI3 for more details).
[b] single point at p/p° = 0.995.
[c] measured by BJH (adsorption branch).

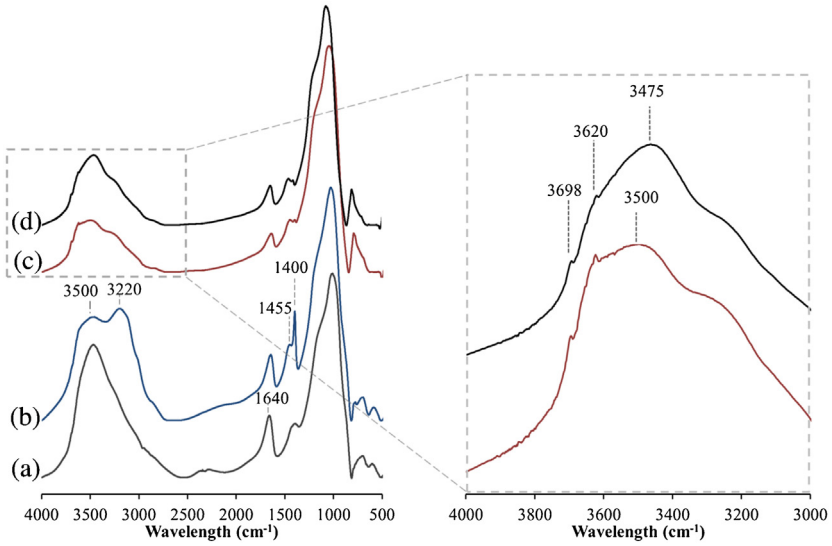

Fig. 5. FTIR spectra of (a) as-prepared Na-hiSi, (b) NH_4^+-ion-exchanged Na-hiSi, (c) after thermal treatment at 450 °C for10 min, (d) Na-hiSi-Seq after thermal treatment at 450 °C for 10 min.

3.2. Ion-exchange and acidity of geopolymer-based catalysts

The ion-exchange process was monitored by FTIR as in Fig. 5, which shows selected spectra of a sequence of Na-hiSi samples throughout the various stages of treatment to produce the catalyst. The initial Na-hiSi sample (Fig. 5a) contains a typical strong broad peak at 1000 cm^{-1} ascribed to the Si-O-Al stretching vibration, with a shoulder at around 1080 cm^{-1} due to the Si-O-Si stretch and another shoulder at about 880 from the Si-OH bending mode [50]. Another small peak at 1400 cm^{-1} arises from carbonate formed by atmospheric carbonation of the geopolymer to form Na_2CO_3, as detected by XRD (Fig. 1). Carbonation is also confirmed by the broad CO_2 asymmetric stretching vibration at about 2347 cm^{-1} [51]. A broad peak at about 3500 cm^{-1} is assigned to hydrogen bonded silanol nests (3500–3400 cm^{-1}) [6–9] while the small peak at 1640 cm^{-1} is due to the H-OH stretching mode from adsorbed water [52]. After ion-exchange with NH_4^+, additional bands appear (Fig. 5b); one at ~3200 cm^{-1} is assigned to the N-H asymmetric stretching vibration, while two other bands at 1455 cm^{-1} and 1400 cm^{-1} are typical bending modes of ammonium ions. Ion exchange is also accompanied by the disappearance of the CO_2 asymmetric stretching band. After heating to 450 °C (Fig. 5c, d), the principal N-H stretching band begins to broaden and only traces remain of the N-H bending modes, resulting from decomposition of the NH_3. The bands at 3500 cm^{-1} and 3475 cm^{-1} are also slightly broadened after thermal treatment due to destruction of the silanol nests. Two new peaks appearing at 3700 cm^{-1} and 3620 cm^{-1} are attributed to H-bonded vicinal silanols and bridging hydroxyls (Bronsted OH) respectively [8,9,36,53]. These weak acidic silanols with minor amounts of Bronsted acid sites are ideal active sites for the Beckmann rearrangement, suggesting that these materials should act as efficient catalysts for this reaction.

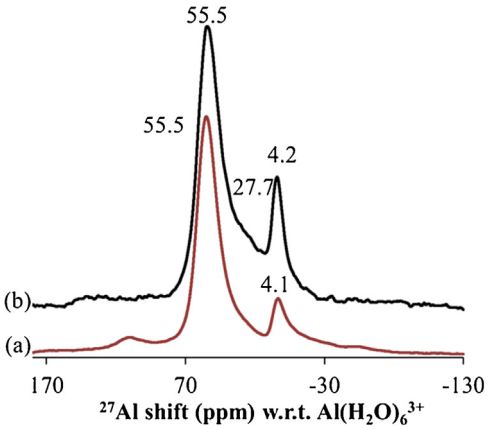

Fig. 6. ^{27}Al MAS NMR spectra of the activated geopolymers. (a) Na-hiSi, (b) Na-hiSi-Seq.

The higher acidity of Na-hiSi-Seq (Table 3) could be ascribed to the higher proportion of EFAl species generated during the thermal pre-treatment. These EFAl species are believed to act as Lewis acid sites in zeolites and zeolite-like materials [54]. This assumption was confirmed by ^{27}Al MAS NMR spectroscopy of both catalysts after thermal treatment at 450 °C for 10 min (Fig. 6). The spectra indicate that the thermal treatment has produced a higher concentration of octahedrally coordinated Al, evidenced by the more intense octahedral resonance at 4.2 ppm and the shoulder at 27.7 ppm arising from 5-coordinated Al associated with the EFAl species.

3.3. Catalytic reactivity

The catalytic performance of the geopolymer-based catalysts for the rearrangement of cyclohexanone oxime to ε-caprolactam is illustrated in Fig. 7. Geopolymer catalysts with low surface area and large pore diameter (K-N, K-hiSi and Na-N, see Table 3) gave the highest conversion of oxime but very low selectivity for ε-caprolactam. The principal by-product resulting from the use of these catalysts was cyclohexanone, due to hydrolysis of the oxime on the Lewis acid sites in the presence of water. Benzamide was also formed as a hydrolysis product of the solvent (PhCN) in a reaction which also requires Lewis acid sites. Traces of other by-products such as of 9-octadecenamide were also detected, resulting from polymerisation side reactions facilitated by the presence of different EFAl species generated during thermal pre-treatment. A possible explanation for these results is that when the surface area is too low, the distribution of the active sites might be very limited and instead of being adsorbed on the surface, the oxime will penetrate into the pores where active sites such as 5- and 6-coordinated EFAl are present and lead to the formation of other by-products. Thus, although the Na-hiSi catalysts with higher surface areas produced slightly lower conversion of oxime compared to the low surface area geopolymer-based catalysts, they showed higher selectivity towards ε-caprolactam.

The influence of the post-synthetic treatment on the textural properties of geopolymer was clearly observed in which the surface area was significantly increased (see Table 3), and consequently affected the selectivity towards ε-caprolactam. As discussed earlier, silanol nests and weakly acidic vicinal silanols are the most likely active sites for this rearrangement. These sites are present in both the Na-hiSi-Seq and Na-hiSi catalysts (Fig. 5); the higher catalytic activity of the former compared to Na-hiSi could be attributed to the higher surface area and hence better distribution of the active sites in the former. These factors facilitate adsorption of the oxime molecules on the catalyst, thereby assisting the rearrangement reaction. The performance of Na-hiSi-Seq was evaluated over a longer time period (Fig. 8); the gradual increase in conversion and selectivity might suggest that saturation of the active sites on the catalyst surface is occurring. If this is the case, the problem might be overcome by running the reaction in a continuous flow system to remove the product as it is formed making available further active sites on which the reaction can occur.

The effect of the reaction temperature and the substrate weight ratio are presented in Fig. 9. The oxime conversion increased significantly from ~33% at 90 °C to ~87% at 140 °C (Fig. 9a). These results are in agreement with the literature and could be attributed to the endothermic nature of Beckmann rearrangement [12,55]. On the other hand, the selectivity to caprolactam was reduced gradually, which is expected as higher temperatures facilitate side reactions leading to the formation of other by-products. Regarding the influence of the oxime: catalyst weight ratio, it can be seen from Fig. 9b that the conversion of the oxime is decreased by reducing the amount of the catalyst. The selectivity to the lactam, however, increased slightly as the amount of by-products obtained decreased. These results could be attributed to the lower amount of active sites responsible for both the rearrangement and production of the by-products. These results are in agreement with those reported for similar experiments with H-USY zeolite [16].

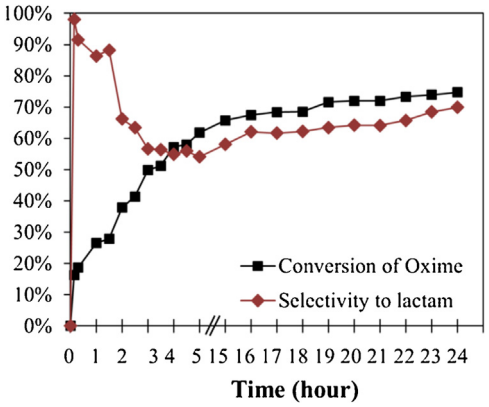

Fig. 8. Catalytic performance of Na-hiSi-Seq as a function of reaction time. Reaction conditions: solvent 20 ml PhCN; 0.1 g catalyst; 0.1 g oxime; T = 130 °C.

The reusability of Na-hiSi-Seq catalysts was studied for up to five reaction cycles and is shown in Fig. 10. As expected, no significant change was observed in the yield of ε-caprolactam; since the active sites are generated within the geopolymer structure, these catalysts do not suffer the drawback of supported catalysts from which the active sites tend to be removed by leaching, deactivating the catalyst and adversely affecting its reusability. The structural stability of the used catalyst, after five recycles, was evaluated by XRD and IR (Figs. 11 and 12). These results show that there is little or no significant change in the spent geopolymer structure, illustrating the stability of the geopolymer-based catalysts.

The performance of the new geopolymer-based catalyst was compared with other commonly used solid catalysts that have been previously reported for the liquid phase Beckmann rearrangement of cyclohexanone oxime. For the most meaningful possible comparison, only those studies are considered in which the reaction conditions were identical to the present work. Since reports of the use of solid catalysts in the liquid phase Beckmann rearrangement are very limited compared with gas-phase systems, only a few studies are available for direct comparison, and these are shown in Table 4. The yield of caprolactam obtained by Na-hiSi-Seq is superior to the H-ZSM-5 and H-Y zeolites tested in this study, and also superior to results reported for tungstated zirconia [18] and Al-MCM-41 [21]. However, Ngamcharussrivichai

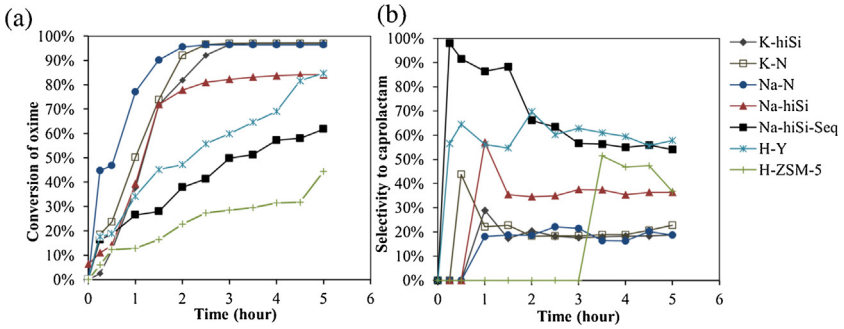

Fig. 7. Catalytic activity of the various geopolymer-based catalysts compared with zeolite catalysts in the Beckmann rearrangement of cyclohexanone oxime to ε-caprolactam. (a) degree of conversion of the oxime, (b) selectivity for the caprolactam product. Reaction conditions: solvent 20 ml PhCN; 0.1 g catalyst; 0.1 g oxime; T = 130 °C.

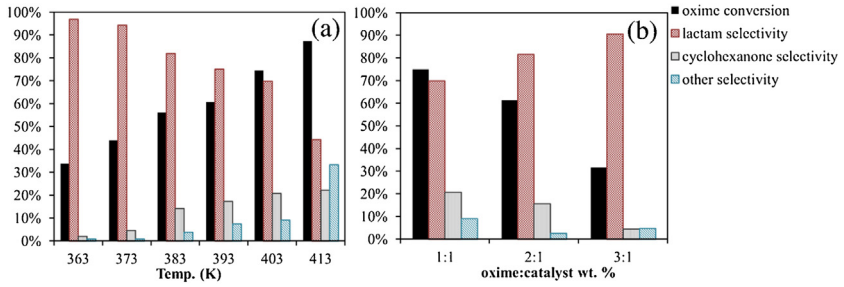

Fig. 9. The influence of the reaction temperature (a), and the oxime: catalyst wt. % (b) on the Beckmann rearrangement reaction. The catalyst is Na-hiSi-Seq, solvent PhCN.

Table 4
Comparison of the catalytic performance of geopolymer-based catalysts with other catalysts for the liquid phase Beckmann rearrangement of cyclohexanone oxime to ε-caprolactam. Reaction conditions: solvent 20 ml PhCN; 0.1 g catalyst; 0.1 g oxime; T = 130 °C; t = 5hr.

Catalyst	Conversion %	Selectivity %			Mass balance %	Ref.
		Lactam	Cyclohexanone	Other		
Na-hiSi	84.08 ± 5.42	36.38 ± 2.75	60.89 ± 1.77	2.73 ± 1.08	97.71	This work
Na-hiSi-Seq[a]	74.70 ± 3.96	69.97 ± 1.95	20.79 ± 0.95	9.24 ± 2.78	98.21	This work
H-Y	84.75 ± 2.67	57.87 ± 0.58	39.93 ± 0.14	2.20 ± 0.86	98.14	This work
H-ZSM-5	44.38 ± 4.95	36.78 ± 2.68	58.82 ± 4.42	4.40 ± 1.74	98.05	This work
$WOxZrO_2$	49.3	79.0				[18]
Al-MCM-41	50.6	89.1				[21]
H-USY	98.0	75.0				[16]

[a] Reaction continued for 24 hours.

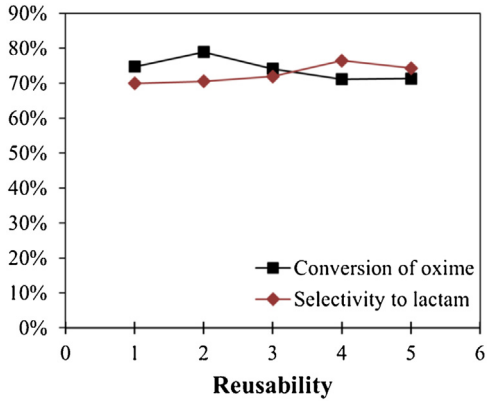

Fig. 10. Reusability of Na-hiSi-Seq over five reaction cycles. Reaction conditions; 1:1:200 oxime: catalyst: solvent wt. %; T = 130 °C; t = 24 hr.

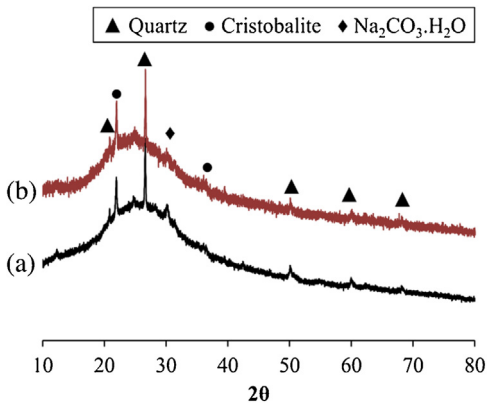

Fig. 11. XRD traces of (a) fresh Na-hiSi-Seq catalyst and (b) the recovered catalyst after five reaction cycles.

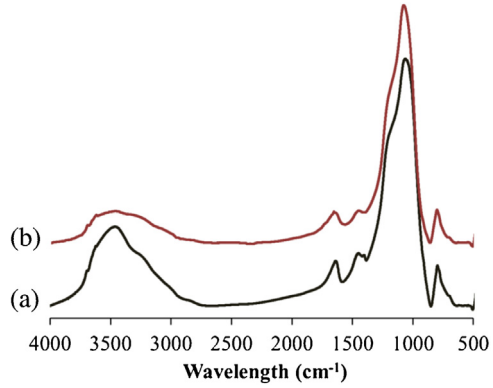

Fig. 12. FTIR spectra of (a) fresh Na-hiSi-Seq catalyst and (b) the recovered catalyst after five reaction cycles heated to 450 °C.

et al. [16] reported a higher yield obtained with ultra-stable Y-zeolite (H-USY). The conversion and selectivity of the geopolymer catalysts can be manipulated by altering their composition and post-synthesis treatments, but in all cases the best performance in this reaction is obtained with the high-silica composition. Moreover, the catalytic activities of the geopolymer-based catalysts are superior to those reported for a wider range of solid catalysts which were tested in liquid phase systems, but under different reaction conditions. These other catalysts include zeolites (large pore Y and beta type [15,16,20]), molecular sieves (Nb-MCM-41 [1] and SBA-15-ar-SO_3H [22]), functionalised silica (H_2SO_4/SiO_2 [24][24a] and $H_2SO_4/M/SiO_2$ [24][24b]), HPAs such as Cs-phosphotungstic acid [19], Fe/Cu-1,3,5-benzenetricarboxylate (MOFs) [20] and ionic liquids (cyanuric chloride in imidazolium-based ILs [25][25a], [Bis-BsImD][$OTf]_2$-$ZnCl_2$] [25][25b] and [C_3SO_3Hmim][Cl–$ZnCl_2$] [25][25c]).

Furthermore, the geopolymer catalysts have the additional advantage of facile synthesis from readily available and relatively inexpensive naturally-occurring raw materials, by comparison with the synthesis of the other advanced catalysts which involves multiple steps and expensive reagents. Since their synthesis does not involve the use of toxic reagents such as OSDAs, geopolymer catalysts are more ecologically-friendly materials. All these factors

suggest that these catalysts represent a new class of materials with advantages in terms of performance, cost, ease of synthesis and ecological friendliness. Further research is required to improve the catalytic performance of these geopolymer-based catalysts; particularly to optimise the post synthetic treatment, as the results of this study indicate the large impact of such treatments on the catalytic reactivity of the geopolymers. It would also be of interest to investigate the application of these catalysts in continuous flow liquid phase or gas phase systems.

4. Conclusion

This study reports the first use of inorganic aluminosilicate geopolymers as heterogeneous solid acid catalysts for the liquid-phase Beckmann rearrangement of cyclohexanone oxime to ε-caprolactam. The geopolymer catalysts are readily prepared at room temperature from natural clay and alkali silicates under alkaline conditions. The catalytic sites are generated within the structure of geopolymer by ion-exchange with NH_4^+ followed by thermal treatment. The surface areas and pore dimensions of the catalysts can be varied by adjusting the starting composition of the inorganic polymers, and it is found that excellent catalytic conversion of the oxime was obtained using geopolymers with small surface areas and large pore diameters; however these catalysts showed low selectivity towards the caprolactam product. This was ascribed to the presence of Lewis acid sites generated by the thermal treatment which produced EFAl species. However, the selectivity towards the ε-caprolactam can be significantly improved by exposing the geopolymer catalysts to a post-synthetic dealumination and desilication treatment which increases the surface area and enhances the distribution of the active sites. The catalytic activity of the geopolymers in the liquid-phase Beckmann rearrangement is superior to, or at least comparable with other solid acid catalysts under identical reaction conditions. These geopolymer-based catalysts were also recycled five times without deterioration in the yield of ε-caprolactam, emphasising their potential as efficient environmentally-friendly inexpensive heterogeneous catalysts as alternatives to the solid acids presently used in Beckmann rearrangement reactions.

Acknowledgements

We are indebted to Grant O'sullivan for supplying the halloysite clay and to David Flynn for assistance with TEM measurements. Mohammad Alzeer acknowledges the financial support of a PhD Fellowship from the MacDiarmid Institute for Advanced Materials and Nanotechnology.

References

[1] M. Anilkumar, W.F. Hoelderich, Appl. Catal. B 165 (2015) 87–93.
[2] J. Zhang, Y. Lu, K. Wang, G. Luo, Ind. Eng. Chem. Res. 52 (2013) 6377–6381.
[3] R.A. Sheldon, I.W.C.E. Arends, U. Hanefeld, Green Chemistry and Catalysis, Wiley-VCH Verlag GmbH & Co. KGaA, 2007, pp. 49–90.
[4] I. Fechete, Y. Wang, J.C. Védrine, Catal. Today 189 (2012) 2–27.
[5] J.H. Clark, Acc. Chem. Res. 35 (2002) 791–797.
[6] G.P. Heitmann, G. Dahlhoff, J.P.M. Niederer, W.F. Hölderich, J. Catal. 194 (2000) 122–129.
[7] B. Bonelli, L. Forni, A. Aloise, J.B. Nagy, G. Fornasari, E. Garrone, A. Gedeon, G. Giordano, F. Trifirò, Microporous Mesoporous Mater. 101 (2007) 153–160.
[8] G.P. Heitmann, G. Dahlhoff, W.F. Hölderich, J. Catal. 186 (1999) 12–19.
[9] J. Kim, W. Park, R. Ryoo, ACS Catal. 1 (2011) 337–341.
[10] E.G. Vaschetto, S.G. Casuscelli, G.A. Eimer, Microporous Mesoporous Mater. 221 (2016) 175–181.
[11] R. Kumar, N. Enjamuri, J.K. Pandey, D. Sen, S. Mazumder, A. Bhaumik, B. Chowdhury, Appl. Catal. A 497 (2015) 51–57.
[12] E. Gianotti, M. Manzoli, M.E. Potter, V.N. Shetti, D. Sun, J. Paterson, T.M. Mezza, A. Levy, R. Raja, Chem. Sci. 5 (2014) 1810–1819.
[13] M. Anilkumar, W.F. Hoelderich, J. Catal. 293 (2012) 76–84.
[14] H. Ichihashi, M. Ishida, A. Shiga, M. Kitamura, T. Suzuki, K. Suenobu, K. Sugita, Catal. Surv. Asia 7 (2003) 261–270.
[15] Y.-M. Chung, H.-K. Rhee, J. Mol. Catal. A: Chem. 175 (2001) 249–257.
[16] C. Ngamcharussrivichai, P. Wu, T. Tatsumi, Appl. Catal. A 288 (2005) 158–168.
[17] M.A. Camblor, A. Corma, H. García, V. Semmer-Herlédan, S. Valencia, J. Catal. 177 (1998) 267–272.
[18] N.R. Shiju, M. AnilKumar, W.F. Hoelderich, D.R. Brown, J. Phys. Chem. C 113 (2009) 7735–7742.
[19] N.R. Shiju, H.M. Williams, D.R. Brown, Appl. Catal. B 90 (2009) 451–457.
[20] M. Opanasenko, M. Shamzhy, M. Lamač, J. Čejka, Catal. Today 204 (2013) 94–100.
[21] C. Ngamcharussrivichai, P. Wu, T. Tatsumi, J. Catal. 227 (2004) 448–458.
[22] X. Wang, C.-C. Chen, S.-Y. Chen, Y. Mou, S. Cheng, Appl. Catal. A 281 (2005) 47–54.
[23] Z. Li, R. Ding, Z. Lu, S. Xiao, X. Ma, J. Mol. Catal. A: Chem 250 (2006) 100–103.
[24] (a) N.C. Marziano, L. Ronchin, C. Tortato, A. Vavasori, C. Badetti, J. Mol. Catal. A: Chem. 277 (2007) 221–232;
(b) N.C. Marziano, L. Ronchin, C. Tortato, A. Vavasori, M. Bortoluzzi, J. Mol. Catal. A: Chem. 290 (2008) 79–87.
[25] (a) A. Maia, D.C.M. Albanese, D. Landini, Tetrahedron 68 (2012) 1947–1950;
(b) X. Liu, L. Xiao, H. Wu, Z. Li, J. Chen, C. Xia, Catal. Commun. 10 (2009) 424–427;
(c) R. Kore, R. Srivastava, J. Mol. Catal. A: Chem. 376 (2013) 90–97.
[26] A.-B. Fernández, A. Marinas, T. Blasco, V. Fornés, A. Corma, J. Catal. 243 (2006) 270–277.
[27] A.B. Fernández, I. Lezcano-Gonzalez, M. Boronat, T. Blasco, A. Corma, J. Catal. 249 (2007) 116–119.
[28] V.R.R. Marthala, Y. Jiang, J. Huang, W. Wang, R. Gläser, M. Hunger, J. Am. Chem. Soc. 128 (2006) 14812–14813.
[29] M.T. Nguyen, G. Raspoet, L.G. Vanquickenborne, J. Am. Chem. Soc 119 (1997) 2552–2562.
[30] J. Perez-Ramirez, C.H. Christensen, K. Egeblad, C.H. Christensen, J.C. Groen, Chem. Soc. Rev. 37 (2008) 2530–2542.
[31] K. Li, J. Valla, J. Garcia-Martinez, ChemCatChem 6 (2014) 46–66.
[32] S. Goel, S.I. Zones, E. Iglesia, Chem. Mater. 27 (2015) 2056–2066.
[33] D. Verboekend, G. Vilé, J. Pérez-Ramírez, Adv. Funct. Mater. 22 (2012) 916–928.
[34] J.L. Provis, G.C. Lukey, J.S.J. van Deventer, Chem. Mater. 17 (2005) 3075–3085.
[35] S.J. O'Connor, K.J.D. MacKenzie, M.E. Smith, J.V. Hanna, J. Mater. Chem. 20 (2010) 10234–10240.
[36] Y.J. Zhang, L. Kang, L.C. Liu, Handbook of Alkali-Activated Cements, Mortars and Concretes, in: J.A. Labrincha, C. Leonelli, A. Palomo, P. Chindaprasirt (Eds.), Woodhead Publishing, Oxford, 2015, pp. 729–775.
[37] O. Bortnovsky, J. Dědeček, Z. Tvarůžková, Z. Sobalík, J. Šubrt, J. Am. Ceram. Soc. 91 (2008) 3052–3057.
[38] B.E. Glad, W.M. Kriven, J. Am. Ceram, Soc. 96 (2013) 3643–3649.
[39] A.T. Durant, K.J.D. MacKenzie, H. Maekawa, Dalton Trans. 40 (2011) 4865–4870.
[40] P. Sazama, O. Bortnovsky, J. Dědeček, Z. Tvarůžková, Z. Sobalík, Catal. Today. 164 (2011) 92–99.
[41] J.R. Gasca-Tirado, A. Manzano-Ramírez, P.A. Vazquez-Landaverde, E.I. Herrera-Díaz, M.E. Rodríguez-Ugarte, J.C. Rubio-Ávalos, V. Amigó-Borrás, M. Chávez-Páez, Mater. Lett. 134 (2014) 222–224.
[42] M. Fallah, K.D. MacKenzie, J. Hanna, S. Page, J. Mater. Sci. 50 (2015) 7374–7383.
[43] S. Sharma, D. Medpelli, S. Chen, D.-K. Seo, RSC Adv. 5 (2015) 65454–65461.
[44] J. Haber, Pure Appl. Chem. 63 (1991) 1227–1246.
[45] V.F.F. Barbosa, K.J.D. MacKenzie, C. Thaumaturgo, Int. J. Inorg. Mater. 2 (2000) 309–317.
[46] J.D.M. Kenneth, E.S. Mark, Pergamon Materials Series Pergamon (2002) 271–330.
[47] R. Baran, Y. Millot, T. Onfroy, J.-M. Krafft, S. Dzwigaj, Microporous Mesoporous Mater. 163 (2012) 122–130.
[48] D. Verboekend, J. Perez-Ramirez, Catal. Sci. Tech. 1 (2011) 879–890.
[49] K.S.W. Sing, D.H. Everett, R.A.W. Haul, L. Moscou, R.A. Pierotti, J. Rouquérol, T. Siemieniewska, Pure Appl. Chem. 57 (1985) 602–619.
[50] W.K.W. Lee, J.S.J. van Deventer, Langmuir 19 (2003) 8726–8734.
[51] A. Zukal, C.O. Arean, M.R. Delgado, P. Nachtigall, A. Pulido, J. Mayerová, J. Čejka, Microporous Mesoporous Mater. 146 (2011) 97–105.
[52] Y. Chen, Z. Guo, T. Chen, Y. Yang, J. Catal. 275 (2010) 11–24.
[53] Y.-J. Ji, H. Xu, D.-R. Wang, L. Xu, P. Ji, H. Wu, P. Wu, ACS Catal. 3 (2013) 1892–1901.
[54] J. Jiao, J. Kanellopoulos, W. Wang, S.S. Ray, H. Foerster, D. Freude, M. Hunger, Phys. Chem. Chem. Phys. 7 (2005) 3221–3226.
[55] D. Mao, Z. Long, Y. Zhou, J. Li, X. Wang, J. Wang, RSC Adv. 4 (2014) 15635–15641.